Fluorescence Spectroscopy of Single Tryptophan Mutants of Apolipophorin-III in Discoidal Lipoproteins of Dimyristoylphosphatidylcholine†

J. L. Soulages* and E. L. Arrese

Department of Biochemistry and Molecular Biology, 355 Noble Research Center, Oklahoma State University, Stillwater, Oklahoma 74078

Received March 30, 2000; Revised Manuscript Received July 3, 2000

ABSTRACT: The structure of the exchangeable apolipoprotein, apolipophorin-III from *Locusta migratoria*, apoLp-III, is described as a bundle of five amphipathic α-helices. To study the interaction of each of the helices of apoLp-III with a lipid surface, we designed five single-Trp mutants, each containing a Trp residue in a different α-helix. The Trp residues were located in the nonpolar domains of the amphipathic α-helices. The kinetics of the spontaneous interaction of the mutants with dimyristoylphosphatidylcholine (DMPC) indicated that all mutants behaved as typical exchangeable apolipoproteins. Circular dichroism in the far-UV indicated that all proteins have a high and similar helical content in the lipid-bound state. The interaction of the Trp residues with the lipid surface was investigated in recombinant lipoprotein particles made with DMPC. The properties of the Trp residues were investigated by fluorescence spectroscopy. These studies showed major changes in the spectroscopic properties of the Trp residues upon binding to lipid. These changes are observed with all single-Trp mutants, indicating that a major conformational change, which affects the properties of all helices, takes place upon binding to lipid. The position of the fluorescence maximum, the quenching efficiency of acrylamide as determined by steady-state and time-resolved fluorescence, and the fluorescence lifetimes of the single-Trp mutants suggest that helices 1, 4, and 5 interact with the nonpolar domains of the lipid. The properties of the Trp in helices 2 and 3 suggest that these helices adopt a different binding configuration than helices 1, 4, and 5. Helices 2 and 3 appear to be interacting with the polar headgroups of the phospholipids or constitute a different domain that does not interact with the lipid surface.

Exchangeable apolipoproteins regulate the metabolism of lipids in animals (*1*−*4*). Apolipophorin-III (apoLp-III)[1] is an exchangeable apolipoprotein found in the hemolymph of many insect species (*5*−*6*). The structure of apoLp-III is described as an up-and-down bundle of five amphipathic α-helices, where the nonpolar sides of the helices are oriented toward the protein core (*7*−*8*).

The study of the structure−function relationship of *Locusta migratoria* apoLp-III is of interest because the knowledge of the crystal structure of apoLp-III offers the possibility of relating the structure of an apolipoprotein to its function. ApoLp-III shares many physical−chemical properties with exchangeable apolipoproteins of humans and other vertebrates (*5*, *9*−*10*). Moreover, the similarity between the properties of insect and vertebrate exchangeable apolipoproteins suggests that elucidation of the mechanism of interaction of apoLp-III with lipids would be useful to the understanding of the function of human apolipoproteins.

On the basis of the crystal structure of apoLp-III and early models developed for human exchangeable apolipoproteins, the accepted model for the lipid-bound state of apoLP-III assumes that the protein spreads on the lipid surface by the movement of helices 1, 2, and 5 in one direction and helices 3 and 4 in the other direction (180°) around "hinges" located in the loops between helices 2 and 3 and between helices 4 and 5 (*7*). A massive interaction of the α-helical domains of apoLp-III with the lipid surface has also been inferred from monolayer adsorption studies (*11*). On the basis of the size, stoichiometry, and geometry of recombinant discoidal lipoproteins particles with dimyristoylphosphatidylcholine (DMPC), it has been proposed that both vertebrate apolipoproteins (*12*−*14*) and insect apolipoproteins adopt an extended conformation interacting with the nonpolar acyl chains of the phospholipid bilayer (*15*). These models are very useful and consistent with the properties of the proteins and the lipoprotein complexes. However, they are not supported by experimental evidence showing the interaction of specific helices with specific domains of the lipid structure.

Taking advantage of the crystal structure of apoLp-III, we have designed and expressed five single-Trp mutants to study the interaction of the helical domains of apoLp-III with a lipid surface. The single-Trp mutants were designed such that the Trp residues resided in the nonpolar side of the amphipathic α-helices. These mutants provided us with a means to study the properties of the helical domains and their interaction with lipid.

† This work was supported by NIH Grant GM 55622 and the Oklahoma Agricultural Experiment Station.

* To whom correspondence should be addressed. Phone: (405) 744-6212; fax (405) 744-7799; e-mail: jose@biochem.okstate.edu.

[1] Abbreviations: Apo, apolipoprotein; apoLp-III, apolipophorin-III; PC, phosphatidylcholine; DMPC, dimyristoylphosphatidylcholine; $K_{s,v}$, Stern−Volmer constant; τ, lifetime.

10.1021/bi0007223 CCC: $19.00
Published on Web 08/03/2000

We have recently reported an extensive characterization of these mutants in the lipid-free state (*16*). In this paper, we present an extensive spectroscopic characterization of these proteins in the lipid-bound state. The properties of the single-Trp mutants were investigated in discoidal recombinant lipoproteins particles made with DMPC. This study revealed interesting differences between the spectroscopic properties of the helical domains. The results obtained suggest that helices 1, 4, and 5 interact with the lipid surface, whereas helices 2 and 3 do not interact with the lipid, or they do it adopting a different binding configuration than helices 1, 4, and 5.

EXPERIMENTAL PROCEDURES

Mutagenesis, Expression, and Purification of the apoLp-III. Site-directed mutagenesis was carried out as previously described (*16*) using the commercial kit, "QuickChange" (Stratagene) and a pET-32a plasmid (Novagen, Madison, WI) containing the insert of *L. migratoria* apoLp-III. Expression of the protein was induced by IPTG, and the thioredoxin−apoLp-III fusion protein was isolated from the bacteria and purified by Ni-affinity chromatography (*17*). Recombinant locust apoLp-III was cleaved from the rest of the fusion protein with enterokinase (Novagen, Madison, WI). ApoLp-III was purified from the cleavage reaction by Ni-affinity chromatography and anionic exchange chromatography in DE52 (Pharmacia).

Circular Dichroism. CD spectra were acquired in a Jasco-715 CD instrument using a 0.1-cm path-length cell. The CD spectra were acquired at 30 °C, every 1 nm with 1 s averaging time per point and a 1-nm band-pass.

Kinetics of the apoLp-III−DMPC Interaction. The kinetics of the apoLp-III−DMPC association was followed by the decrease in absorbance at 325 nm that accompanies the transformation of the multilamellar liposomes into discoidal lipoprotein particles as described by Pownall et al. (*18*). The reactions were performed at 23.9 °C in a Hewlett-Packard diode array spectrophotometer equipped with a temperature-controlled cell holder. A 10:1 lipid to protein molar ratio was used. The reaction was started by the addition of 50 μL of a liposome suspension (2.5 mg of DMPC/mL) to 1950 μL of an apoLp-III solution in 20 mM Tris buffer at pH 7.9 equilibrated at 23.9 °C. Data acquisition was started 10 s after the addition of the liposomes.

Fluorescence Spectroscopy. Lifetime studies were performed using a multifrequency phase and modulation fluorometer model K-2 (ISS, Urbana, IL) using a 300-W xenon lamp as excitation source. The light was modulated between 2 and 200 MHz by Pockells cell modulator. The excitation was set up at 295 nm and polarized at 35° by a Glan-Thompson prism polarizer. The emission was collected through a 335WG filter (Schott Inc.). A solution of *p*-terphenyl in absolute ethanol was used as lifetime reference ($\tau = 1$ ns). The fluorescence intensities of the samples were matched to the intensity of the reference by changing the concentration of *p*-terphenyl. Data were collected at 15 different frequencies and analyzed by nonlinear least squares using the ISS software. Different decay models were fitted assuming a multiexponential decay law. For each lifetime model, the best fitting parameters were obtained by minimization of the reduced χ^2 value (*19*). All measurements were carried out at 30 °C, and the samples were in 20 mM Tris buffer, pH 7.8. These experiments were carried out using 0.4-cm path length cells. Uncorrected tryptophan fluorescence spectra and integrated intensities were recorded with an ISS K2 fluorescence spectrophotometer.

Fluorescence quantum yields were measured relative to a 1.6 μM solution of tryptophan in 5 mM sodium phosphate buffer, pH 7, assuming a quantum yield for free Trp of 0.14 at 20 °C (*20*). The integrated areas, λ: 300−450 nm, of the corrected fluorescence spectra of the samples were compared to the integrated intensity of the Trp solution. The excitation wavelength was 280 nm, at which the optical densities of the solutions did not exceed 0.025.

In all fluorescence quenching experiments, the initial absorbance of the sample was below 0.025. Aliquots of acrylamide (7 M in water) were added in microliter amounts directly to the sample. The samples were excited at 295 nm using 0.5-mm slits for the excitation and emission monochromators (8-nm bandwidth). The emission was collected between 305 and 400 nm every 1 nm. Fluorescence data were corrected for the Raman peak of the solvent. Minor corrections were also performed to account for the dilution and the inner filter effect arising from the additions and the absorption of acrylamide ($\epsilon^{295} = 0.23\ M^{-1}\ cm^{-1}$).

Fluorescence anisotropy was measured with excitation and emission monochromators set up at 295 and 340 nm, respectively. Data were corrected for the contribution of the buffer and the instrumental G factor.

Preparation of the Lipoprotein Complexes. Discoidal recombinant particles were obtained by the cholate dialysis method (*21*). DMPC was dispersed in 20 mM Tris buffer, pH 7.9, containing 150 mM NaCl and sodium cholate. An aliquot of the DMPC dispersion was mixed with the protein such that the final molar ratio of cholate/DMPC/protein was 350:135:1. The samples were dialyzed four times against 4 L of buffer (total 16 L) during 8−12 h periods (approximately 48 h).

The heterogeneity and size of the lipoproteins were determined by gradient gel electrophoresis (*22*) in 3.5−20% polyacrylamide gels. The electrophoresis was performed in Tris-Borate buffer, pH 8.8, for 30 h at 4 °C and 130 V. High molecular weight markers (Pharmacia) were use for size calibration. Sizes were estimated using as reference the distance migrated by LDH and a plot of 1/diameter vs R_f.

RESULTS

To identify the domains of the apoLp-III that interact with the lipid surface, we need to have reporter groups in all the protein domains that are being investigated. One of the less perturbing methods for the incorporation of probes resides in the selective replacement of amino acid residues by tryptophan, which constitutes an excellent and versatile spectroscopic probe. To simplify the experiments and the interpretation of the results, it is preferable to have only one Trp residue per molecule of apoLp-III that will be studied. On the basis of the crystal structure of the *L. migratoria* protein and attempting to introduce the least number of perturbations in the protein, the following set of five single-Trp mutants was designed: Ile19Trp (reporter of helix 1), Phe49Trp (helix 2), Phe78Trp (helix 3), and Leu135Trp (helix 5). The wild-type apoLp-III contains Trp 113 in helix

Table 1: Kinetics, Secondary Structure, and Steady-State Fluorecence Properties of the Single-Trp Mutants of apoLp-III in Complexes with DMPC

	Trp-helix 1	Trp-helix 2	Trp-helix 3	Trp-helix 4	Trp-helix 5
rate const (min^{-1})[a]	0.60 ± 0.01	0.54 ± 0.07	0.38 ± 0.05	0.41 ± 0.05	0.69 ± 0.06
α-helix %[b]	62	51	56	54	55
λ_{max} (nm)[c]	330 ± 2	337 ± 1	338 ± 2	323 ± 1	325 ± 2
Φ_F 30 °C[d]	0.208	0.201	0.194	0.290	0.212
fluores aniso[e] 30 °C	0.133	0.157	0.160	0.149	0.135
18 °C	0.149	0.169	0.171	0.166	0.140

[a] Pseudo-first-order rate constants for the spontaneous formation of recombinant lipoproteins of apoLp-III-DMPC. Data obtained at 23.9 °C. [b] The α-helical content was estimated by the method of Chen and Yang (*30*). The error in these determinations is of the order of 10% and arises from the estimation of the protein content. [c] The position of the fluorescence emission maxima represents the average value ± SE of four different recombinant lipoprotein preparations. [d] Quantum yields were measured as indicated in Experimental Procedures. [e] The standard errors of the anisotropy of fluorescence ranged between 0.001 and 0.003.

4 and Trp 128 in the loop connecting helices 4 and 5. Therefore, apoLp-III molecules containing Trp in the helices 1, 2, 3, and 5 were constructed by mutating the double mutant Trp128Phe/Trp113Phe, which contains no Trp. To obtain the mutant containing a reporter Trp in helix 4, at position 113, a single mutation was required (Trp128Phe). In all these mutants, the Trp residues were located in the hydrophobic side and near the middle of the amphipathic α-helices.

Lipid−Protein Interaction. All mutants were tested for apolipoprotein activity using as a model system the interaction of the proteins with multilamellar liposomes of DMPC. The kinetics of the association of the recombinant single-Trp mutants of *L. migratoria* apoLp-III with DMPC was studied at 23.9 °C. The interaction of DMPC with exchangeable apolipoproteins is characterized by a decrease in light scattering due to the disruption of the large liposomes and the formation of small discoidal apolipoprotein−DMPC particles (*18*). All proteins interacted with DMPC promoting the formation of discoidal apoLp−lipid complexes. Figure 1 shows the turbidity decays obtained during the first 15 min of the reaction for all five mutants. The apparent pseudo-first-order rate constants are included in Table 1. The rate constants show some differences among the mutants. However, similarly to the kinetics of the wild-type protein (*17*), all proteins showed a fast reaction with DMPC, indicating that the mutations did not have a major impact on the lipid-binding activity of the proteins.

Even though apoLp-III spontaneously formed discoidal particles upon the interaction with DMPC, the spectroscopic studies were carried out with discoidal lipoproteins obtained by the cholate dialysis method (*20*). Using this method, we did not need to work with an excess of lipid-free apolipoprotein and were able to obtain discoidal lipoproteins that were free of unbound apolipoprotein. The size of the lipoprotein complexes was determined by gradient gel electrophoresis (*21*). The most abundant lipoprotein complex (~80%) obtained with all mutants has an average diameter of 18 nm. A similar size was previously reported for discoidal particles obtained with wild-type apoLp-III (*15*, *23*). Two other minor bands with estimated sizes 20 and 15 nm were also present in the preparations.

The α-helical content of the proteins in the lipid-bound state was studied by circular dichroism. All proteins have typical spectra of α-helical peptides with minima at 208 and 222 nm (Figure 2) and α-helical contents ranging between 50 and 60% (Table 1).

Fluorescence Spectra. The position of the maximum in the fluorescence emission spectra of Trp provides an excellent means to study the polarity of the environment of the indole group. Residues in a highly polar environment have a maximum around 354 nm, and those residues in a highly nonpolar environment display a maximum near 310 nm (*24*). The position of the maximum (Table 1 and Figure 3) indicates that, in the lipid-bound state, the Trp residues of all helical domains reside in an environment of intermediate polarity (λ_{max}: 324−338 nm). For each Trp mutant, only minor variations in the position of the maximum were observed among different preparations of recombinant lipoproteins. The Trp residues in helices 2 and 3 have a fluorescence maximum that was consistently red-shifted to the maximum observed for the Trp residues in helices 1, 4, and 5. This difference suggests that the residues in helices 2 and 3 reside in an environment of slightly higher polarity. The fluorescence maximum for the Trp residue in helix 4 indicates that this residue is located in a milieu of lower polarity than the remaining residues.

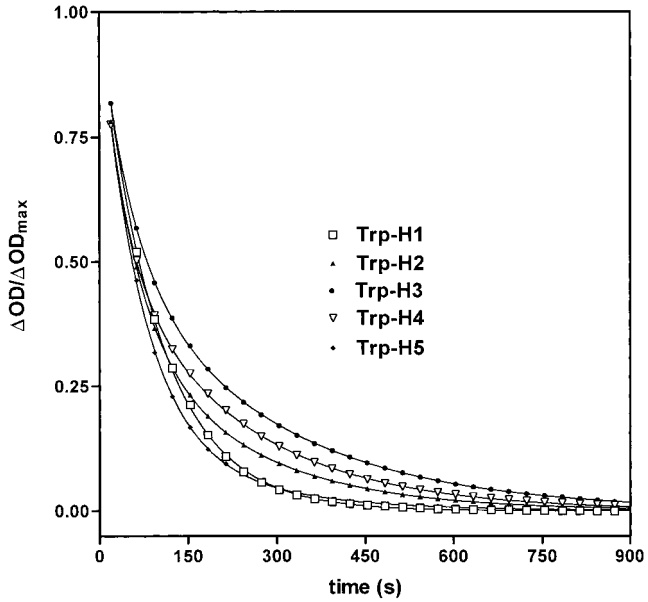

FIGURE 1: Kinetics of the association of the single-Trp mutants of apoLp-III with multilamellar liposomes of DMPC. The experimental conditions are indicated in Experimental Procedures. Trp-H1, Trp-H2, Trp-H3, Trp-H4, and Trp-H5 refer to the mutants containing a single Trp residue in helices 1, 2, 3, 4, and 5, respectively. Reactions were performed at 23.9 °C.

Wild-type apoLp-III contains one Trp residue in helix 4(W113), the same as that present in the single-Trp mutant W128F, and a Trp residue in position 128, which is located in the loop connecting the helices 4 and 5. In DMPC

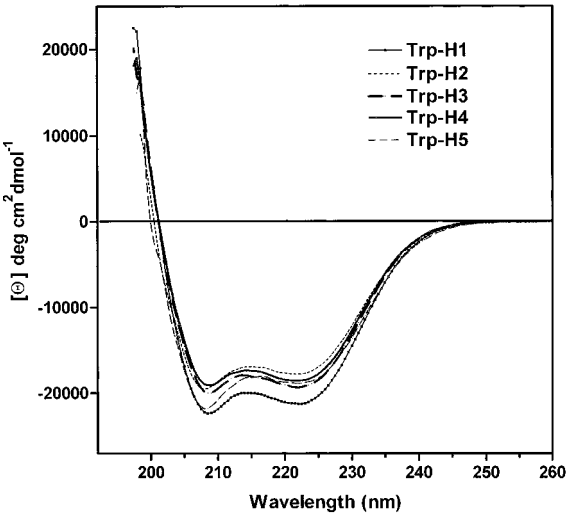

FIGURE 2: Far-UV Circular Dichroism of the single Trp mutants in discoidal particles of DMPC. The lipoproteins were in 5 mM sodium phosphate, pH 7.9, containing 250 mM NaCl, and the spectra were acquired at 30 °C. Symbols are indicated in the figure. Trp-H1, Trp-H2, Trp-H3, Trp-H4, and Trp-H5 refer to the mutants containing a single Trp residue in helices 1, 2, 3, 4, and 5, respectively.

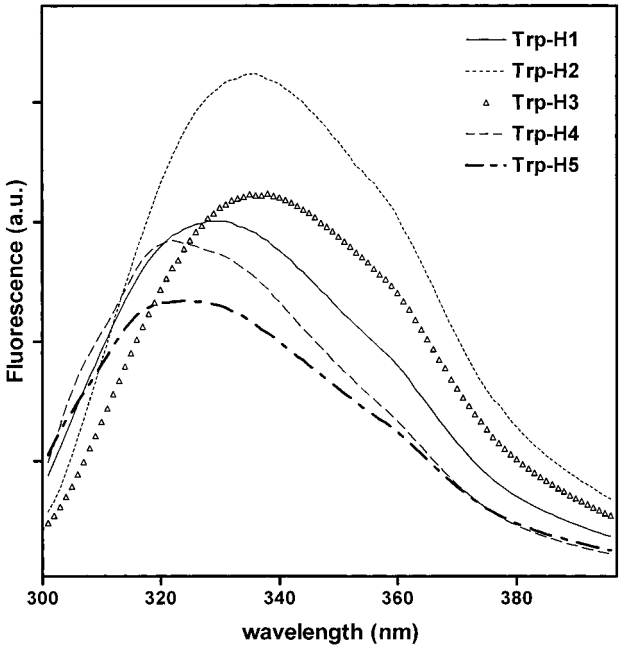

FIGURE 3: Fluorescence emission spectra of the single-Trp mutants in discoidal particles of DMPC. The fluorescence emission spectra were obtained at 30 °C in buffer 20 mM Tris, pH 7.9. The excitation monochromator was set up at 280 nm. Symbols are indicated in the figure.

complexes, the wild-type protein has a fluorescence maximum at 332 nm (*17*). The comparison between the maximum observed in the wild-type protein and that of the W128F mutant suggests that the fluorescence maximum of the Trp residue 128 is located at a wavelength longer than 332 nm. Therefore, this residue appears to reside in a milieu of higher polarity than the Trp residues located in helices 1, 4, and 5.

Quantum Yields. The fluorescence quantum yield of the single-Trp mutants in the lipid-bound state is indicated in Table 1. Only small differences are observed among the quantum yields of Trp residues in helices 1, 2, 3, and 5. The Trp in helix 4 has the highest quantum yield (0.29), which is nearly 50% higher than the quantum yields of the Trp in any of the other helices (∼0.19−0.20). When the proteins are unfolded (2 M Gdn HCl), the fluorescence quantum yield of the Trp mutants is 0.11. Using the quantum yield of the unfolded proteins, we can compare the quantum yields of the lipid-bound mutants to the quantum yields of lipid-free mutants recently reported (*16*). The comparison indicates that lipid binding induces an increase (40%) in the fluorescence of the mutant containing a Trp residue in helix 5. The Trp residue in helix 4 has the highest quantum yield in both the lipid-free and the lipid-bound states. However, as compared to the lipid-free form, its quantum yield is reduced by nearly 50% in the lipid-bound state. On the other hand, lipid binding did not promote significant changes in the quantum yields of the Trp residues located in helices 1, 2, and 3.

Fluorescence Lifetimes. The fluorescence lifetime of the single-Trp mutants was determined by frequency-domain fluorescence spectroscopy. The decays were well described by a major contribution to the intensity of a long lifetime, 4−5 ns component, and a minor contribution from a fast-decaying component in the range of 1 to 2 ns (Table 2). The contribution of scattering ($\tau = 0$ ns) to the light intensity did not exceed 10%. The contribution of scattering was included in the global fitting of the modulation and phase data. From these multiexponential decays, we calculated the mean lifetimes (Table 2). The Trp residues in helices 4 and 5 have the shortest mean lifetimes, whereas the Trp residues in helices 2 and 3 have the longest lifetimes. Similar results were obtained in two separate experiments, performed with independently prepared lipoprotein complexes.

Fluorescence Anisotropy. The intrinsic anisotropy of fluorescence depends on the segmental motions of the Trp residues and their lifetimes. Given the large size of the discoidal lipoprotein particles, the fluorescence anisotropy could only be slightly affected by the long rotational correlation time of the entire particle. The values of steady-state anisotropy of fluorescence obtained for each of the single-Trp mutants in the lipid-bound state are shown in Table 1. The results indicate that the Trp residues in helices 1, 4, and 5 have a higher mobility than the Trp residues in helices 2 and 3. Because the Trp residues in helices 2 and 3 have the highest mean lifetimes of fluorescence, the differences observed in fluorescence anisotropy cannot be due to differences in lifetime. Thus, the results indicate a higher mobility of the Trp residues in helices 1, 4, and 5. To explore the effect of the mobility of the acyl chains on the mobility of the Trp residues, we determined the anisotropies of fluorescence determined at 18 and 30 °C. For all the Trp mutants, a small increase in the anisotropy of fluorescence of Trp is observed when the temperature is reduced. This increase in anisotropy appears to affect all the Trp residues to about the same extent.

Fluorescence Quenching. Acrylamide quenching of the intrinsic Trp fluorescence was used to determine the accessibility of the Trp residues in each of the α-helical domains. Acrylamide is polar but uncharged and has good access to all but the most deeply buried tryptophan residues (*25*). Steady-state measurements indicate that all residues are significantly protected from the aqueous media. In the concentration range of quencher used in this study, all Stern−Volmer plots were linear (Figure 4). The apparent $K_{s,v}$ values of the Trp mutants bound to DMPC are shown in Table 2.

Table 2: Lifetime and Acrylamide Quenching of Trp Fluorescence: Comparison among the Single-Trp Mutants in the Lipid-Bound State

	Trp-helix 1		Trp-helix 2		Trp-helix 3		Trp-helix 4		Trp-helix 5	
	τ_1	τ_2	τ_1	τ_2	τ_1	τ_2	τ_1	τ_2	τ_1	τ_2
lifetimes (ns)[a]	5.84	2.33	4.89	1.03	5.92	1.61	4.53	1.61	4.62	1.20
fraction	0.57	0.36	0.89	0.08	0.74	0.20	0.69	0.25	0.73	0.15
χ^2	8		7		9		19		10	
$\langle\tau_o\rangle$ ns exp 1	4.48		4.57		5.00		3.75		4.03	
exp 2	4.40		4.59		5.05		3.57		4.00	
steady-state $K_{s,v}$ (M^{-1}) average $K_{s,v}$ value[b]	2.46 ± 0.59		3.76 ± 1.38		3.41 ± 0.71		2.17 ± 0.27		2.08 ± 0.77	
time-resolved $K_{s,v}$ (M^{-1})	0.915 ± 0.026		1.860 ± 0.034		2.336 ± 0.099		0.812 ± 0.021		0.898 ± 0.027	
k_q (from τ) (M^{-1} ns^{-1})[c]	0.20		0.41		0.47		0.22		0.22	

[a] Data were fitted to a three-component multiexponential decay assuming that the third lifetime was constant and equal to zero. The small contribution of this lifetime would account for the scattering. The fractions of this lifetime were low and can be inferred from the table. Lifetimes were determined at an excitation wavelength of 295 nm using a WG335 emission filter. A *p*-terphenyl solution in ethanol was used as lifetime reference. The fluorescence intensities of the samples were matched to the intensity of the reference by changing the concentration of *p*-terphenyl. [b] Steady-state apparent $K_{s,v}$ values were obtained by fitting the data to the Stern−Volmer quenching equation. Data represent the average of three independent experiments ± SD. [c] k_q values were obtained from the lifetimes corresponding to experiment 1.

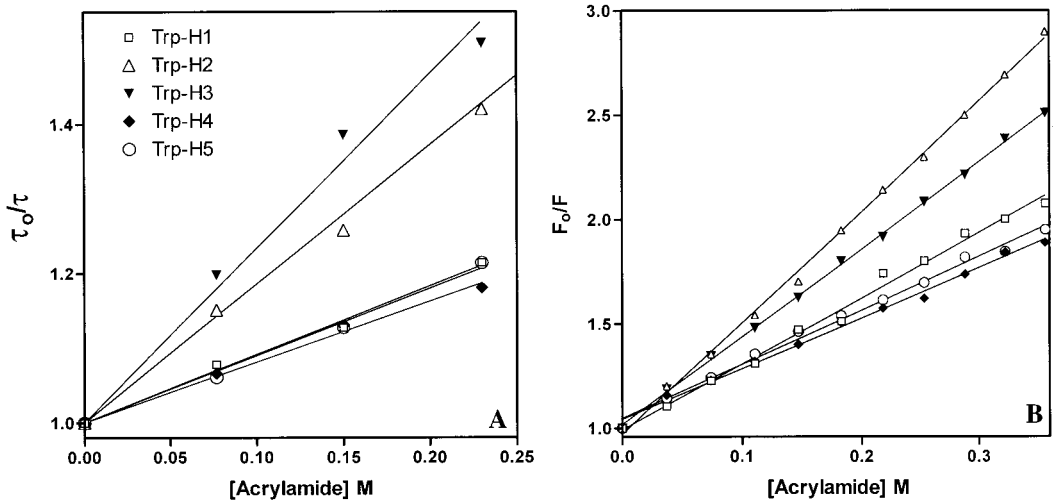

FIGURE 4: Acrylamide quenching of DMPC-bound single Trp mutants. Panel A shows the Stern−Volmer plots obtained in steady-state fluorescence quenching studies. Panel B shows the plots constructed with the lifetime data. Experimental conditions are given in Experimental Procedures. Symbols are indicated in the figure.

The differences between the quenching efficiency of acrylamide for different mutants are significantly large. The steady-state experiments were repeated with independent preparations of lipoproteins. The average results indicate that the Trp residues in helices 2 and 3 are approximately 40 to 80% more accessible to the quencher than the Trp residues in helices 1, 4, and 5.

To distinguish the contributions from dynamic and static quenching, the accessibility of the Trp residues was also studied by time-resolved fluorescence. Figure 4 (panel B) shows the relative change in the fluorescence lifetime as a function of the concentration of acrylamide. The absolute values of the apparent $K_{s,v}$ are higher than the lifetime-derived $K_{s,v}$ values. This is almost always the case and is due to the contribution of distance-dependent quenching processes (*26*). However, consistently with the steady-state results, the $K_{s,v}$ values recovered from the time-resolved measurements also indicate a higher exposure of the Trp residues in helices 2 and 3. The estimated collisional quenching constants indicate that the Trp residues in helices 2 and 3 are approximately 100% more accessible than the Trp residues in helices 1, 4, and 5.

DISCUSSION

Apolipophorin-III constitutes an excellent model system for exploring the molecular basis of the interaction of exchangeable apolipoproteins with lipid surfaces. ApoLp-III from *Manduca Sexta* and *L. migratoria* represent the best characterized insect apolipoproteins (*5*−*6*). The fact that the NMR structure of *M. Sexta* apoLp-III (*8*) and the crystal structure of *L. migratoria* apoLp-III (*7*) have been determined provides an excellent opportunity to design studies directed to address the relationship between structure and function of exchangeable apolipoproteins.

To understand the function of exchangeable apolipoproteins, we need to know the structure of the lipid-free protein as well as the structure of the protein in the lipid-bound state. As compared to the lipid-free state, there is very little information about the conformation of apoLp-III in the lipid-bound state.

The principal goal of this work is to obtain information related to the role of each of the five helical domains of apolipophorin-III in the lipid−protein interaction. To this purpose, we have explored the optical spectroscopic properties of five single-Trp mutants in the lipid-bound state using

a well-known model lipoprotein system. The mutations were designed such that the Trp residues would be located in the nonpolar face of the helices. This decision was based on the model of interaction of amphipathic helices with phospholipids (*10*) and the broadly accepted idea that, upon binding to lipid, apoLp-III adopts an open conformation where the hydrophobic faces of the α-helices interact with the acyl chains of the phospholipid along the periphery of the discoidal particles (*15*, *22*).

Changes in the Properties of the Trp Residues upon Binding to Lipid. We have recently studied the spectroscopic properties of the same five single-Trp mutants in the lipid-free state (*16*). The position of the maximum of the fluorescence spectra of the Trp mutants is shifted in all the mutants upon binding to lipid. However, the direction of the change is different depending on the location of the residue. The Trp residues located in helices 1 and 5 undergo an important blue shift of 29 and 8 nm, respectively. On the other hand, the Trp residues located in helices 2, 3, and 4 are red-shifted 20, 5, and 12 nm, respectively. The differences between the properties of the Trp residues in the lipid-free and lipid-bound states suggest that a major conformational change is taking place upon binding to lipid. Our study can be compared to a recent fluorescence study of single-Trp mutants located in the N-terminal domain of human apoA-I (*28*). Contrasting with apoLp-III, a comparison of the fluorescence spectra of lipid-free and lipid-bound single-Trp mutants of apoA-I always showed a small blue shift in the lipid-bound forms. On the other hand, the range of λ_{max} values observed in the lipid-bound state was similar among the apoLp-III and the apoA-I mutants. The position of λ_{max} falls between 330 and 336 nm for the single-Trp mutants of apoA-I and between 323 and 338 nm for the apoLp-III mutants.

A comparison of the collisional quenching constants for acrylamide between the lipid-free (*16*) and the lipid-bound mutants indicates that, independently of the shift on the position of the fluorescence spectra, all Trp residues have a lower acrylamide accessibility in the lipid-bound state. This is markedly evident for the Trp residues in helices 1 and 5 whose k_q values are reduced to 15% of the values for the free proteins (∼6-fold reduction). This large decrease is because the Trp residues in helices 1 and 5 are the most exposed residues in the lipid-free protein. On the other hand, as compared to the lipid-free state, the decrease in k_q values of the Trp residues located in helices 2, 3, and 4 only represents between a 1.5- and 2-fold reduction. The modest decrease in k_q values for these residues does not mean that the Trp residues are less exposed than in the lipid-free protein. The extent of the decreases in k_q values observed for the Trp resides in helices 2, 3, and 4 could be explained by the trivial effect of the increased macromolecular size on the quenching constants (*27*).

The lifetime of the mutant containing a Trp residue in helix 4 is nearly the same in both the lipid-free ($\tau = 3.90$ ns) and the lipid-bound states ($\tau = 3.75$ ns). However, the mean fluorescence lifetimes of the remaining single-Trp mutants of apoLp-III are approximately 30% longer in the lipid-bound state than in the lipid-free state. In a spectroscopic study of single-Trp mutants of human apoA-I, Davidson et al. (*28*) also found an increase in the mean lifetimes upon binding of the protein to lipid. The increase in lifetime is interesting because, in general, it is not accompanied by an increase in quantum yield. Although we have not studied the mechanism of depopulation of the excited state, the longer lifetimes observed in the lipid-bound state could be due to restricted access of the solvent to the fluorophore and the lower rate of collisional quenching by the lipid molecules when compared to the water molecules. The fact that the fluorescence quantum yields, in most cases, decrease or remain constant upon binding to lipid could imply a significant static-quenching mechanism by the lipid molecules. Obviously, further studies will be needed to address these observations.

Comparison between the Properties of the Trp Residues in the Lipid-Bound State. The fluorescence properties of the single-Trp mutants showed consistent differences between the properties of some of the helices. According to the experimental data, helices 2 and 3 display similar properties, and these are clearly different from the fluorescent properties found for the mutants containing a Trp residue in helices 1, 4, and 5. The fluorescence spectra of the Trp in helices 1, 4, and 5 are blue-shifted as compared to the spectra of the Trp in helices 2 and 3. These differences in the spectra suggest that the environment of the Trp residues in helices 1, 4, and 5 has a lower polarity than the environment of the Trp residues in helices 2 and 3. One possible interpretation of these differences would be that the Trp residues in helices 1, 4, and 5 are interacting with the acyl chains of the phospholipid, whereas helices 2 and 3 would constitute a two-helix domain that would not interact with the lipid. It is also possible that helices 2 and 3 interact with a more polar region of the lipid structure, such as that of the polar headgroups of the phospholipid or their polar/hydrocarbon interface. A correlation between the position of the fluorescence spectra and the location of the Trp residues in a bilayer was reported for α-helical peptides containing a single-Trp residue (*27*). Peptides interacting with the hydrocarbon region of the bilayer have a fluorescence spectrum that is blue-shifted when compared to the spectra of peptides interacting with polar/hydrocarbon interface of the bilayer (*29*). In discoidal lipoproteins of DMPC and apolipoproteins, the phospholipids appear to be arranged in a bilayer structure (*4*). This is also the case for recombinant lipoproteins obtained with apoLp-III (*15*). The stability of this type of lipid structure is provided by the interaction of the apolipoprotein with the acyl chains of the phospholipid molecules along periphery of the discoidal particle. This assumption is valid, but it does not mean that all helices of the apolipoprotein should interact with the acyl chains. Some of the helices could be interacting with the polar headgroups of the phospholipid bilayer. Extending the rationale derived from the study by Ren et al. (*29*), the Trp residues in helices 4 and 5 would be embedded near the middle of the lipid bilayer of the discoidal particle, whereas the Trp residue in helix 1 would reside near the interface formed by the acyl chains and polar headgroups of the phospholipid.

Additional differences between helices were observed by fluorescence anisotropy, fluorescence lifetime, and quenching of the Trp fluorescence. These studies also revealed that the properties of the Trp residues in helices 2 and 3 have significant differences with the properties of the Trp residues located in helices 1, 4, and 5. The mobility of the Trp residues in helices 1, 4, and 5 is higher and their lifetimes are shorter

than those of Trp residues in helices 2 and 3. The shorter lifetimes confirm that the lower anisotropy of fluorescence of the Trp in helices 1, 4, and 5 is not due to a longer lifetime. The higher mobility of the Trp residues in helices 1, 4, and 5 could be due to their interaction with the hydrocarbon region that extends along the periphery of the discoidal particles.

Steady-state and time-resolved fluorescence quenching experiments indicated that the Trp residues in the three-helix group are less exposed to the quencher than the Trp residues in helices 2 and 3. Altogether, the blue shift, the lower solvent exposure, and the higher mobility of the Trp residues in helices 1, 4, and 5 suggest that these helices would be interacting with the acyl chains of the phospholipid.

Conclusions. Although the models of interaction of apo-Lp-III with phospholipid have assumed that all helices interact with the lipid surface, the evidence to support the model is considerably weak. The major support for the model arises from the area occupied by apoLp-III at the air−water interface (*11*) and the size and stoichiometry of the discoidal lipoprotein particles obtained with DMPC (*15*). The large differences between the spectroscopic properties of lipid-free mutants recently characterized (*16*) and the properties of the mutants in the lipid-bound state determined in this study suggest that a large conformational change is taking place upon binding to lipid.

The results of this study suggest that helices 1, 4, and 5 are interacting with the lipid surface. On the other hand, the higher accessibility to the quencher and the relative red shift of the fluorescence maximum of the Trp residues in helices 2 and 3 are not consistent with a tight lipid−helix interaction. It is possible that in the lipid-bound state helices 2 and 3 constitute a two-helix protein domain that does not interact with the lipid surface. It is also possible that these two helices interact with the polar headgroups of the phospholipids. Clearly, additional studies will be needed to confirm the role of the α-helices of apoLp-III in the lipid−protein interaction.

REFERENCES

1. Fielding, C. J., and Fielding, P. E. (1995) *J. Lipid Res. 36*, 211−228.
2. Atkinson, D., and Small, D. M. (1986) *Ann Rev. Biophys. Chem. 15*, 403−456.
3. Phillips, M. C., Gillotte, K. L., Haynes, M. P., Johnson, W. J., Lund-Katz, S., and Rothblat, G. H. (1998) *Atherosclerosis 137*, S13−17.
4. Pownall, H. J., and Gotto, A. M., Jr. (1992) in *Structure and Function of Apolipoproteins* (Rosseneu M., Ed.) pp 1−32. CRC Press, Boca Raton, FL.
5. Narayanaswami, V., and Ryan, R. O. (2000) *Biochim. Biophys. Acta 1483*, 15−36.
6. Soulages, J. L., and Wells, M. A., (1994) *Adv. Prot. Chem. 45*, 371−415.
7. Breiter, D. R., Kanost, M. R., Benning, M. M., Wesemberg, G., Law, J. H., Wells, M. A., Rayment, I., and Holden, H. M. (1991) *Biochemistry, 30*, 603−608.
8. Wang, J., Gagné, S. M., Sykes, B. D., and Ryan, R. O. (1997) *J. Biol. Chem. 272*, 17912−17920.
9. Smith, A. F., Owen, L. M., Strobel, L. M., Chen, H. D. R., Kanost, M. R., Hanneman, E., and Wells, M. A. (1994) *J. Lipid Res. 35*, 1976−1984.
10. Segrest, J. P., Jones, M. K., de Loof, H., Brouillette, C. G., Venkatachalapathi, Y. V., and Anantharamaiah, G. M. (1992)- *J. Lipid Res. 33*, 141−166.
11. Kawooya, J. K., Meredith, S. C., Wells, M. A., Kezdy, F. J., and Law, J. H. (1986) *J. Biol. Chem. 261*, 13588−13591.
12. Pownall, H. J., Massey, J. B., Sparrow, J. T., and Gotto, A. M., Jr. (1987) in *Plasma Lipoproteins* (Gotto, A. M., Jr., Ed.) pp 95−127, Elsevier Science Publishers B. V., Amsterdam.
13. Segrest, J. P., Jones, M. K., Klon, A. E., Sheldahl, C. J., Hellinger, M., De Loof, H., and Harvey, S. C. (1999) *J. Biol. Chem. 274*, 31755−31758.
14. Raussens, V., Fisher, E., Goormaghtigh, E., Ryan, R. O., and Ruysschaert, J.-M. (1998) *J. Biol. Chem. 273*, 10953−10960.
15. Wientzek, M., Kay, C. M., Oikawa, K., and Ryan, R. O. (1994) *J. Biol. Chem. 269*, 4605−4612.
16. Soulages, J. L., and Arrese, E. L. (2000) *J. Biol. Chem. 275*, 17501−17509.
17. Soulages, J. L., Pennington, J., Bendavid, O., and Wells, M. A. (1998) *Biochem. Biophys. Res. Commun. 243*, 272−276.
18. Pownall, H. J., Massey, J. B., Kusserow, S. K., and Gotto, A. M., Jr. (1978) *Biochemistry 17*, 1183−1188.
19. Lakowicz, J. R., Lazko, G., Cherek, H., Limkeman, M., and Gratton, E. (1984) *Biophys. J. 46*, 463−477.
20. Chen, R. F. (1967) *Anal. Lett. 1*, 35−42.
21. Jonas, A., Kezdy, K. E., and Wald, J. H. (1989) *J. Biol. Chem. 264*, 4818−4824.
22. Nichols, A. V., Krauss, R. M., and Musliner, T. A. (1986) *Methods Enzymol. 128*, 417−431.
23. Weers, P. M. M., Kay, C. M., Oikawa, K., Wientzek, M., Van der Horst, D. J., and Ryan, R. O. (1994) *Biochemistry 33*, 3617−3624.
24. Burstein, E. A., Vedenkina, N. S., and Ivkova, M. N. (1973) *Photochem. Photobiol. 18*, 263−279.
25. Kurzban, G. P., Gitlin, G., Bayer, E. A., Wilchek, M., and Horowitz, P. M. (1989) *Biochemistry 28*, 8537−8542.
26. Lakowicz, J. R., Zelent, B., Gryczynski, I., Kusba, J., and Johnson, M. L. (1994) *Photochem. Photobiol. 60*, 205−214.
27. Johnson, D. A., and Yguerabide, J. (1985) *Biophys. J. 48*, 949−955.
28. Davidson, W. S., Arnvig-McGuire, K., Kennedy, A., Kosman, J., Hazlett, T. L., and Jonas, A. (1999) *Biochemistry 38*, 14387−14395.
29. Ren, J., Lew, S., Wang, Z., and London, E. (1997) *Biochemistry 36*, 10213−10220.
30. Chen, Y., and Yang, J. T. (1971) *Biochem. Biophys. Res. Commun. 44*, 1285−1289.

BI0007223